GFZ
Helmholtz-Zentrum
POTSDAM

Originally published as:

Olwendo, O. J., Cesaroni, C., Yamazaki, Y., Cilliers, P. (2017): Equatorial ionospheric disturbances over the East African sector during the 2015 St. Patrick's day storm. - *Advances in Space Research*, *60*, 8, pp. 1817—1826.

DOI: http://doi.org/10.1016/j.asr.2017.06.037

Equatorial ionospheric disturbances over the East African sector during the 2015 St. Patrick's Day storm

Olwendo O. J[1]., C. Cesaroni[2], Y. Yamazaki[3] , P. Cilliers[4,5]

1. Pwani University, School of Pure and Applied Sciences, Department of Mathematics and Physics, P.O Box 195-80108, Kilifi, Kenya. *castrajoseph@yahoo.com.
2. Istituto Nazionale di Geofisica e Vulcanologia, 00143 Roma Italia.
3. GFZ German Research Centre for Geosciences, Potsdam, Germany, yamazaki@gfz-potsdam.de.
4. South African National Space Agency, Space Science Directorate, P.O Box 32, Hermanus, South Africa. pjcilliers@sansa.or.za.
5. Department of Electrical Engineering, University of Cape Town, Private Bag, Rondebosch 7701, South Africa.

Abstract

During solar cycle 24, the St. Patrick's Day storm on 17 March, 2015 was one of the most severe geomagnetic storms. Several research investigations have been done and are still ongoing about this storm since the dynamics of this storm differs on a global scale from one sector to another. We study the response of the equatorial ionosphere to the storm in the East African sector. Total electron content (TEC) data from ground stations are used to examine the evolution of the Equatorial Ionization Anomaly (EIA) during the storm. The TEC observations show a reduced EIA during 18-20 March 2015, consistent with previous studies at other longitudes. Analyses of ground magnetometer data and the thermospheric composition data from the NASA/TIMED satellite reveal the reduced EIA observed following the storm is due to the combined effect of the disturbance dynamo and composition change.

1.0 Introduction

The equatorial and low latitude ionosphere is characterized by the existence of the daytime Equatorial Ionization Anomaly (EIA) and post-sunset formation of equatorial plasma bubbles. The EIA is produced by the equatorial ionospheric fountain effect at the dip equator which is formed by daytime eastward electric fields [Appleton, 1946; Rishbeth, 2000]. The eastward

electric fields together with the almost horizontal north-ward directed B-field produce an upward E x B vertical drift which lifts the plasma to higher altitudes from where it diffuses to higher latitudes along magnetic field lines. The diffusion of the plasma to higher latitudes creates ionization crests on both sides of the magnetic equator at about ± 15^{o} magnetic latitudes [Kelley, 2009].

During strong geomagnetic activity, a large amount of energy is deposited into the high latitude ionosphere. This results in an enhancement of electric fields and currents at high latitudes, which causes Joule heating. The resulting disturbance winds can influence the global pattern of ionospheric electric fields and currents, through the process known as disturbance dynamo [Blanc and Richmond, 1980]. The disturbance dynamo, along with the penetration of the high-latitude electric fields to lower latitudes, can significantly disturb the equatorial ionosphere during geomagnetic storms [Fejer and Scherliess, 1997; Sastri et al., 2000]. The electric fields generated by the storm can be identified as the short-lived prompt penetration electric field and a longer lasting disturbance dynamo electric field originating from the solar wind magnetospheric dynamo [Kelly et al., 2003; Richmond et al., 2003; Maruyama et al., 2005; Lin et al., 2007]. The penetration electric field is eastward during daytime and westward during night, and it can last only a few hours [Fejer and Scherliess 1997; Lin et al., 2007]. The disturbance dynamo electric field tends to oppose the quiet time zonal electric field, thus westward during daytime and eastward during night. It can last for more than a day. Consequently, the daytime eastward electric field can increase or decrease during a storm, which would result in a stronger and weaker plasma fountain, respectively.

The St. Patrick's Day storm on 17 March 2015 is one of the most severe geomagnetic storms of solar cycle 24, and has drawn great attention of researchers. This particular storm has been studied using various measurement techniques which include in situ observations from satellites and ground based monitoring equipments on a global scale. For example, Ramsingh et al. (2015) examined the response of the equatorial and low-latitude ionosphere over the Indian sector, using magnetometer, ionosonde, and GPS data. Another study by Tulasi et al., [2016] for instance used a set of in situ observation from SWARM-A and SWARM-C satellites and a chain of ionosondes

at different longitudes. In their study, they compared the zonal electric field response to the eastward convection electric field induced by the storm. Their findings indicated that there was a large upward surge of the equatorial F-layer which subsequently led to the development of spread F in the Indian sector. This observation was attributed to the equatorial zonal electric field enhancement by the penetration of the eastward electric field at dusk. In the Indonesian sector which was only ~15 degrees apart from the Indian sector Tulasi et al., [2016] reports that the observations were contrary to that on the Indian sector. Also another study at the low latitude and mid-latitude on a global scale on the St. Patrick's day storm has been reported by Nava et al., [2016]. In their study, they also used different instruments including ground based and satellite based. Their study revealed that there were differences in response to the storm from the three sectors of their study namely the African, American and Asian sectors. For example, they observed the strongest positive storm effect in VTEC in the American sector which was on the night side on 17 March 2015 and a negative storm effect in VTEC in African longitudinal sector at the middle and high latitudes. The St. Patrick's day storm response of the low latitude ionosphere in the South-East Asian sector is deeply investigated by Spogli et al., [2016] in which the authors analyzed ground based and space born electron density and magnetic data. They found a huge depletion of TEC with respect to the quiet behavior, in both the crests and trough regions at the beginning of the recovery phase of the storm (18 March). Other studies about this storm in high latitude regions can also be found in Astafyeva et al., [2015] and Cherniak and Zakharenkova [2015]. We investigate the response of the equatorial ionosphere to the St. Patrick's Day in the East African sector based on a unique data set.

2.0 Data and Analysis

2.1 Total Electron Content (TEC)

The GNSS data used for this research were obtained from the UNAVCO database (http://www.unavco.org/). We use the data from the stations located in the East African region within the latitudinal range from 20˚S to 30˚N (see Figure 1 for the locations of the GNSS station used in this study). We examine the period 15 to 22 March 2015. The Vertical Total Electron

Content (VTEC) were computed from the RINEX observation files using the VTEC calibration technique developed by Ciraolo et al., [2007] and also described in Cesaroni et al. [2015].

2. 2 Ground-based magnetometer data

The storm time ionospheric electrodynamics has been investigated using the measurement of ionospheric disturbance currents. The disturbances currents arise from the penetration of the disturbance electric field from the Polar Regions and/or from disturbance winds generated by enhanced Joule heating at high latitudes. The ionospheric disturbance currents were computed using the horizontal (H) component of the geomagnetic field at Addis Ababa (Mag 0.9□N), near the magnetic equator, and the magnetic field in Hermanus (Mag 42.6□S). It is assumed that the horizontal component comprises a superposition of signals that can be described as follows:

$$H = C + SV + Sq + D_I + D_M ,$$

where C is the permanent crustal magnetization (Purucker and Whaler, 2007); SV is the main magnetic field and its secular variation due to the Earth's core dynamo process (Finlay et al., 2012); Sq is the contribution of the solar-quiet (Sq) current system due to the ionospheric wind dynamo (Yamazaki and Maute, 2016); D_I is the effect of disturbance ionospheric currents; D_M is the contribution by magnetospheric currents. The subtraction of the nighttime data largely removes the magnetic fields associated with C and SV. The Sq field, derived as the average daily variation during the five quietest days of the month, can also be removed from the data. The residual magnetic perturbation, defined here as;

$$\Delta H = D_I + D_M$$

We plot in Figure 2 the residual magnetic perturbations at Addis Ababa (ΔH_{AAE}) and Hermanus (ΔH_{HER}). The two curves show similar variations, indicating the dominance of the magnetospheric effect D_M. Since Addis Ababa and Hermanus are located in the same longitude sector, the magnetospheric contributions D_M are approximately the same at the two stations. Meanwhile, the ionospheric effects D_I can be different at the two locations, because D_I is much enhanced at Addis Ababa due to the Cowling effect, which is effective only at the magnetic equator (e.g., Kikuchi et al., 1996; Zaka et al., 2009). Therefore, the difference between ΔH_{AAE} and ΔH_{HER} represents the contribution of ionospheric disturbance currents, which are amplified at the Addis Ababa location. It is noted that D_I arises not only from solar-wind disturbances but

also from forcing due to tides and other atmospheric waves from the lower atmosphere (Yamazaki et al., 2014). This explains small differences between ΔH_{AAE} and ΔH_{HER} during quiet periods.

As shown in the paper by Yamazaki and Maute (2016, pp 33), 1 nT of the geomagnetic perturbation roughly corresponds to 1 mA/m of ionospheric currents, which is used for the unit conversion in this study. It should be noted that the parameter D_I is expected to vary with the strength of the equatorial electrojet (EEJ), which is conventionally derived as the difference in H at an equatorial station and a low-latitude station located several degrees away from the magnetic equator (Rastogi and Patil, 1986; and many others). We do not attempt to calculate the conventional EEJ strength since there is no suitable low-latitude station in the East African region during the storm event.

2.3 Thermospheric composition

We also use the thermospheric composition derived from the Global Ultraviolet Imager (GUVI) on board NASA's Thermosphere, Ionosphere, and Mesosphere, Energetics and Dynamics (TIMED) satellite. The TIMED/GUVI provides the column-integrated $[O]/[N_2]$ ratio, where [O] and $[N_2]$ represent the density of the atomic oxygen and molecular nitrogen, respectively. Since the main production mechanism of the F-region O^+ plasma is the photoionization of atomic oxygen O and the main loss mechanism of O^+ involves a reaction with molecular species such as N_2 and O_2, the O^+ density tends to vary with the $[O]/[N_2]$ ratio. Therefore, the $[O]/[N_2]$ data can provide insight into the influence of the thermospheric composition on the ionospheric plasma density variability during the storm. Previous studies on the thermospheric composition from the TIMED/GUVI revealed significant variability in the $[O]/[N_2]$ ratio during storm periods [e.g., Zhang et al., 2004; Meier et al., 2005; Crowley et al., 2006].

3.0 Results

3.1 Interplanetary magnetic indices variations during storm

In this section we highlight the key events associated with the evolution of this storm. In **Figure 3(a)** we show the interplanetary parameters namely the solar wind speed Vx, the interplanetary

magnetic field Bz and the average magnetic field B, during the period prior to and after the storm spanning through 10 to 25 March 2015. The interplanetary electric fields (IEF) and the SymH are presented alongside in **Figure 3(b)**.

Details of the storm evolution can be found in all the references pertaining to the St. Patrick day storm mentioned earlier. We therefore only summarize the key events in relation to the electrodynamic process associated with this storm. As indicated in **Figure 3(a)** the rapid rise of the solar wind speed to nearly 500 km/s followed by a further increase to values above 500 km/s on 17 March marked the onset of the main phase of the storm. Over the same time period there were very strong magnetic activity levels for the entire day as marked by the |B| values of nearly 30 nT. A North directed IMF B_z turning to South on 17 March does coincide with the strong negative excursion of the SYM-H. The SYM-H was however interrupted by the IMF B_z turning North between 09:00 UT and 12:00 UT. Subsequently the negative values of SYM-H remained high at values of about -200 nT up to nearly the end of 17 March.

3.2 Equatorial ionsopheric plasma density variations

Our observation of Total Electron Content (TEC) from a network of stations spanning between latitudes of 20°S and 30°N through the East African Sector (in the longitudinal range of 36°E and 46°E) was used to evaluate the impact of this storm on the ionization levels. Figure 4 depicts the latitudinal distribution of TEC over the East African sector during 15-25 March 2015. The basic latitudinal structure of the EIA with two ionization peaks is clearly visible during daytime. The northern and southern crests can be seen at ~20°N and ~5°S, respectively. As detailed in our previous paper [Olwendo et al., 2015], the plasma density in this longitudinal sector peaks around 1100 UT (1300 LT) and remains significant until around 1800 UT (2000 LT).

The storm effect on the equatorial ionospheric plasma is most evident during 18-20 March 2015 (i.e., the recovery phase of the storm). During this period, the double-hump structure of the EIA was weak, and the overall ionization was lower compared to the period before the storm (15-16 March 2015). Moreover, the latitude extent of the EIA was reduced, which is especially

noticeable in the Southern Hemisphere where the crest shifted equatorward from -5˚S (15-16 March) to 0˚ (18-20 March). All these observations are consistent with the weakening of the equatorial plasma fountain [e.g., Balan and Bailey, 1995].

3.2 Equatorial ionospheric disturbance currents

Figure 5 shows the difference between ΔH_{AAE} and ΔH_{HER}, which represents the disturbance ionospheric current superposed on the quiet-time current. The results are presented for the period 16 to 20 March (i.e the period a day prior to the storm; and three days into the recovery phase of the storm). The gap in the plot after 18 March indicates a lack of data during the period.

The noontime disturbance current was nearly zero on 16 March before the storm event began. The existence of a westward disturbance ionospheric current may be inferred from the daytime results during the storm, from 17 through 20 March 2015. It is noted, however, that the westward disturbance current on 17 March extends into the nighttime hours, when ionospheric currents are considered to be insignificant due to low ionospheric conductivities. Thus, this could be a spurious effect due to contaminations of non-ionospheric contributions. It is known that the magnetospheric ring current is zonally asymmetric during severe storms, especially during the first ~24 hrs from the onset (Newell and Gjerloev, 2012). Although the longitudinal separation between Addis Ababa and Hermanus is small (approximately 20˚), we cannot rule out the possibility that ΔH_{AAB}-ΔH_{HER} is contaminated by the effect of the asymmetric ring current during the main phase. We, thus, refrain from interpreting the disturbance current on 17 March.

The daytime disturbance current was westward during 18-20 March, which is consistent with previous studies that found a westward disturbance current during the recovery phase of a storm (e.g., Yamazaki and Kosch, 2015). The westward disturbance current is considered to be due to the disturbance dynamo electric field (Blanc and Richmond, 1980) that opposes the quiet-time eastward field during daytime and thus weakens the equatorial plasma fountain. Thus, the weak EIA observed during 18-20 March 2015 (Figure 4) can be attributed, at least in part, to the disturbance dynamo effect.

The gradual decay of the westward disturbance current can be seen during 18-20 March. The noontime westward disturbance current intensity, marked by the red dots in Figure 5, decreased from ~100 mA/m on 18 March to ~50 mA/m on 20 March. From this, one might expect a steady recovery of the EIA from 18 March to 20 March. Contrary to this expectation, the overall ionization level on 18 March was higher than the following two days (Figure 4). These results suggest that the time evolution of the EIA during the recovery phase cannot be explained solely by the disturbance dynamo effect.

3.3 Thermospheric composition during the storm

Figure 6 shows the thermospheric composition over the African sector during 16-20 March 2015. The results for 16 March represent a pre-storm condition, while the results for 17 March represent the thermospheric composition a few hours after the storm onset. A sudden increase in the SYM-H index at 0445 UT (Figure 3b) indicates the arrival of the coronal mass ejection (CME) to the Earth's magnetosphere. The results for 18-20 March correspond to the recovery phase of the storm.

It can be seen in Figure 6 that there was an enhancement in the $[O]/[N_2]$ ratio at equatorial latitudes during the recovery phase of the storm. This enhancement was accompanied by a reduction of the $[O]/[N_2]$ ratio middle latitudes, especially in the Southern Hemisphere. The $[O]/[N_2]$ ratio over the equatorial region was highest on 18 March and gradually decreased in the following days (19 and 20 March). This gives an explanation to the higher plasma density on 18 March compared to 19 and 20 March.

4.0 Discussion and Conclusion

In this paper we analyzed the electrodynamics of the ionospheric TEC and the disturbances in electric fields during the severe magnetic storm on St. Patrick's Day 2015. This storm can be traced to 17 March when a Coronal Mass Ejection hit the Earth at about 04:45 UT. This

particular storm remains one of the largest of solar cycle 24 and with very peculiar and unique characteristics. Other than being one of the largest since 2005, this storm occurred without any prior significant precursors such as X or M-class solar flares [Kamide and Kusano, 2015]. The storm is characterized by two strong successive southward turning IMF B_z events on 17 March followed by a long gradual recovery phase starting from 18 March as shown in **Figures 3a and 3b**.

The response of the Equatorial Ionization Anomaly to the storm have been analyzed using a set of ground-based TEC data spanning different latitudes along the East African longitudinal sector. Our analysis of the TEC data revealed a reduced EIA structure during the recovery of phase the storm (18-20 March), consistent with previous reports for other longitudinal sectors [Nava et al., 2016; Nayak et al., 2016]. Ground magnetometer data indicated a westward disturbance ionospheric current during this period, which is probably due to the westward disturbance dynamo electric field. The reduced TEC during the recovery phase is consistent with the weakening of the equatorial plasma fountain due to the disturbance dynamo effect. However, the disturbance dynamo effect on the equatorial plasma fountain alone cannot explain the time evolution of the EIA. For example, the overall ionization level at equatorial latitudes was higher on 18 March than on 19 and 20 March, while the disturbance dynamo effect was strongest on 18 March. Such an inconsistency indicates that other mechanisms also played a role for the TEC variability during the storm. The thermospheric composition derived from the TIMED/GUVI revealed an enhancement in the $[O]/[N_2]$ ratio on 18 March, which explains relatively high plasma density on 18 March.

Based on these results we conclude that two mechanisms played a role in the TEC response to the St. Patrick's Day storm in the African sector. One is the reduction of the equatorial plasma fountain due to the westward disturbance dynamo electric field during daytime, and the other is the enhanced O^+ plasma production due to changes in the thermsopheric composition. Both effects need to be taken into account to fully explain the evolution of the EIA during the storm.

Acknowledgements

The authors would like to thank the University Navstar Consortium (UNAVCO), and the Coordinated Data Analysis Web (CDAWeb) for allowing access to their websites for GPS data and interplanetary magnetic parameter data respectively. The results presented in this paper rely on the data collected at Addis Ababa and Hermanus magnetic observatories. We thank Geophysical Observatory of Addis Ababa University and the South African National Space Agency in Hermanus for supporting its operation and INTERMAGNET for promoting high standards of magnetic observatory practice (www.intermagnet.org)..

References

Anderson, D., A. anghel, K. Yumoto, M. Ishitsuka, E. Kudeki, Estimating daytime vertical E x B drift velocities in the equatorial F-region using ground-based magnetometer observation, Geophys. Res. Lett., 29, 12, 1596, 10.1029/2001GL014562, 2002.

Anderson, D., A. Anghel, J. Chau, and O. Veliz, Daytime vertical E x B drift velocities inferred from ground-based magnetometer observations at low latitudes. Space Weather, 2, S11001, doi:10.1029/2004SW000095, 2004.

Appleton, E. V., Two anomalies in the ionosphere, Nature, 157, 691, 1946.

Astafyeva, E., I. Zakharenkova and M. Forster, Ionospheric response to the 2015 St. Patrick's Day storm: A global multi-instrumental overview, J. Geophys. Res., Space Physics, 120, 9023-9037, doi:10.1002/2015JA021629, 2015.

Balan, N., and G. J. Bailey, Equatorial plasma fountain and its effects: Possibility of an additional layer, J. Geophys. Res., 100,21,421–21,432, 1995.

Blanc, M., and A. D. Richmond, The ionospheric disturbance dynamo, J. Geophys. Res. 85, 1669-1688, 1980.

C. Cesaroni, L. Spogli, L. Alfonsi, G. De Franceschi, L. Ciraolo, et al., L-band scintillations and calibrated total electron content gradients over Brazil during the last solar maximum, J. Space Weather Space Clim., 5, A36, 2015.

Cherniak, I., and I. Zakharenkova, Dependence of the high-latitude plasma irregularities on the auroral activity indices: a case study of 17 March 2015, geomagnetic storm, Earth, Planet and Space, 67: 151, doi:10.1186/s40623-015-0316-x, 2015.

Ciraolo, L., F. Azpilicueta, C. Brunini, A. Meza, and S. M. Radicella, Calibration errors on experimental slant total electron content (TEC) determined with GPS, J. Geod. 81, 111-120, 2007.

Fejer, B. G. and L. Scherliess, Time dependent response of equatorial ionospheric electric fields to magnetospheric disturbances, Geophys. Res. Lett., 22 (7), 851-854, 1995.

Fejer, B. G., and L. Scherliess, Empirical models of storm time equatorial zonal electric fields, J. Geophys. Res., 102, 24047-24056, 1997.

Finlay, C. C., Jackson, A., Gillet, N., and Olsen, N., Core surface magnetic field evolution 2000–2010. Geophysical Journal International, 189(2), 761-781, 2012.

Kamide, Y., and K. Kusano, No major solar flares but the largest geomagnetic storm in the present solar cycle, Space Weather 13, 365-367, 2015.

Kelly, M. C., 2009. The Earth's Ionosphere plasma physics and electrodynamics. International Geophysics series 96.

Kelley, M. C., J. I. Makela, J. L. Chau, and M. J. Nicolls, Penetration of the solar wind electric field into the magnetospheric/ionospheric system, Geophys. Res. Lett., 30(4), 1158, 2003.

Kikuchi, T., Lühr, H., Kitamura, T., Saka, O., and Schlegel, K., Direct penetration of the polar electric field to the equator during a DP 2 event as detected by the auroral and equatorial magnetometer chains and the EISCAT radar. Journal of Geophysical Research: Space Physics, 101(A8), 17161-17173, 1996.

Le Huy, M., C. Amory-Mazaudier, Planetary magnetic signatures of the storm wind disturbance dynamo currents: D_{dyn} J. Geophys. Res. 113, A02312, doi:10.1029/2007JA012686, 2008.

Lin, C-H., J-Y. Liu, H-F. Tsai, and C-Z. Cheng, Variations in the equatorial Ionization anomaly peaks in the western pacific region during the geomagnetic storms of April 6 and July 15, 2000, Earth Planets Space, 59, 401-405, 2007.

Maruyama, N., A. D. Richmond, T. J. Fuller-Rowell, M. V. Codrescu, S. Sazykin, F. R. Toffoletto, R. W. Spiro, and G. H. Millward, Interaction between direct penetration and disturbance dynamo electric electric fields in the storm-time equatorial ionosphere, Geophys. Res. Lett., 32, L17105, 2005.

Nava, B., J. Rodríguez-Zuluaga, K. Alazo-Cuartas, A. Kashcheyev, Y. Migoya-Orué, S. M. Radicella, C. Amory-Mazaudier, and R. Fleury, Middle and low latitude ionosphere response to 2015 St. Patrick's Day geomagnetic storm, J. Geophys. Res. Space Physics, 121, 3421-3438, doi:10.1002/2015JAO22299, 2016.

Nayak, C., L.-C. Tsai, S.-Y. Su, I. A. Galkin, A. T. K. Tan, E. Nofri, and P. Jamjareegulgarn, Peculiar features of the low-latitude and midlatitude ionospheric response to the St. Patrick's Day geomagnetic storm of 17 March 2015, J. Geophys. Res., 121, 7941–7960, 2016.

Olwendo, O. J., Y. Yamazaki, P. Cilliers, P. Baki, C. M. Ngwira, C. Mito, A study on the response of equatorial Ionization Anomaly over the East African sector during the geomagnetic storm of November 13, 2012. Adv. Space Res., 55, 2863-2872, 2015.

Olwendo, O. J., Y. Yamazaki, P. J. Cilliers, P. Baki and P. Doherty, A study on the variability of ionospheric total electron content over the East Africa low latitude region and storm time Ionospheric variations. Radio Sci., 51, doi:10.1002/2015RS005785.

Purucker, M. E. and Whaler, K. A.: Crustal magnetism, in: Geomagnetism, Volume 5, Treatise on Geophysics, edited by: Kono, M., pp. 195–235, Elsevier Science, New York, NY, 2007.

Ramsingh, S. Sripathi, S. Sreekumar, S. Banola, K. Emperumal, P. Tiwari, and B. S. Kumar, Low-latitude ionosphere response to super geomagnetic storm of 17/18 March 2015: Results from a chain of ground- based observations over Indian sector, J. Geophys. Res. Space Physics, 120, 10,864–10,882, doi:10.1002/ 2015JA021509, 2015.

Rastogi, R.G. and A. Patil, Complex structure of equatorial electrojet current. Curr. Sci. 55, 433-436, 1986.

Richmond, A. D., C. Peymirat, and R. G. Roble, long-lasting disturbance in the equatorial ionospheric electric field simulated with a coupled magnetosphere-ionosphere-thermosphere model, J. Geophys. Res., 108(A3), 1118, 2003.

Rishbeth, H., The equatorial F-layer: progress and puzzles, Ann. Geophys., 18, 730, 2000.

Sastri, J. H., et al., Ionospheric storm of early November 1993 in Indian equatorial region, J. Geophys Res., 105, 18443-18455, 2000.

Spogli, L., Cesaroni, C., Di Mauro, D., Pezzopane, M., Alfonsi, L., Musicò, E., ... & Linty, N., Formation of ionospheric irregularities over Southeast Asia during the 2015 St. Patrick's Day storm, J. Geophys. Res. Space Physics, 121, doi:10.1002/2016JA023222, 2016.

Tulasi, R. S., et al., Duskside enhancement of equatorial zonal electric field response to convection electric fields during the St. Patrick's Day Storm on 17 March 2015, J. Geophys. Res. Space Physics, 121, 538-548, doi:10.1002/2015JA021932, 2016.

Verkhoglyadova, O. P., B. T. Tsurutani, A. J. Mannucci, M. G. Mlynczak, L. A. Hunt, L. J. Paxton and A. Komjathy. Solar wind driving of ionosphere thermosphere response in three storms near St. Patrick Day in 2012, 2013 and 2015. J. Geophys. Res. Space Physics, 121, doi:10.1002/2016JA022883.

Prolss, G. W. (1995), Ionospheric F region storms Hand book of Atmospheric electrodynamics, CRC Press, Boca, Raton, Fla.

Yamazaki, Y., A. D. Richmond, A. Maute, H.-L. Liu, N. Pedatella, and F. Sassi, On the day-to-day variation of the equatorial electrojet during quiet periods, J. Geophys. Res. Space Physics, 119, doi:10.1002/2014JA020243, 2014.

Yamazaki, Y., and M. J. Kosch, The equatorial electrojet during geomagnetic storms and substorms, J. Geophys. Res. Space Physics, 120, doi:10.1002/2014JA020773, 2015.

Yamazaki, Y. and A. Maute, Sq and EEJ—A review on the daily variation of the geomagnetic field caused by ionospheric dynamo currents. Space Sci. Rev., 1-107, doi:10.1007/s11214-016-0282-z, 2016.

Zaka, K. Z., A. T. Kobea, P. Assamoi, K. O. Obrou, V. Doumbia, K. Boka, B. J.-P. Adohi, and N. M. Mene, Latitudinal profile of the ionospheric disturbance dynamo magnetic signature: Comparison with the DP2 magnetic disturbance, Ann. Geophys., 27, 3523–3536, 2009.

Figure 1: Geographical locations of the stations used to generate the Total Electron Content maps. The black dots represent the locations of the receivers used in this study. The red line represents the geomagnetic equator.

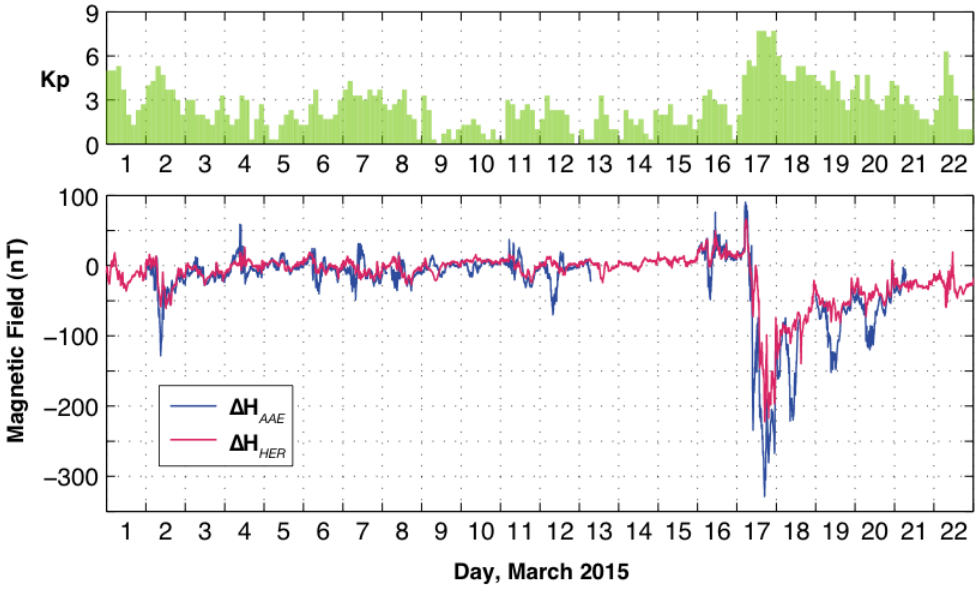

Figure 2: (Top) The Kp index during 1-22 March 2015. (Bottom) The residual magnetic perturbations at Addis Ababa (ΔH_{AAE}) and Hermanus (ΔH_{HER}).

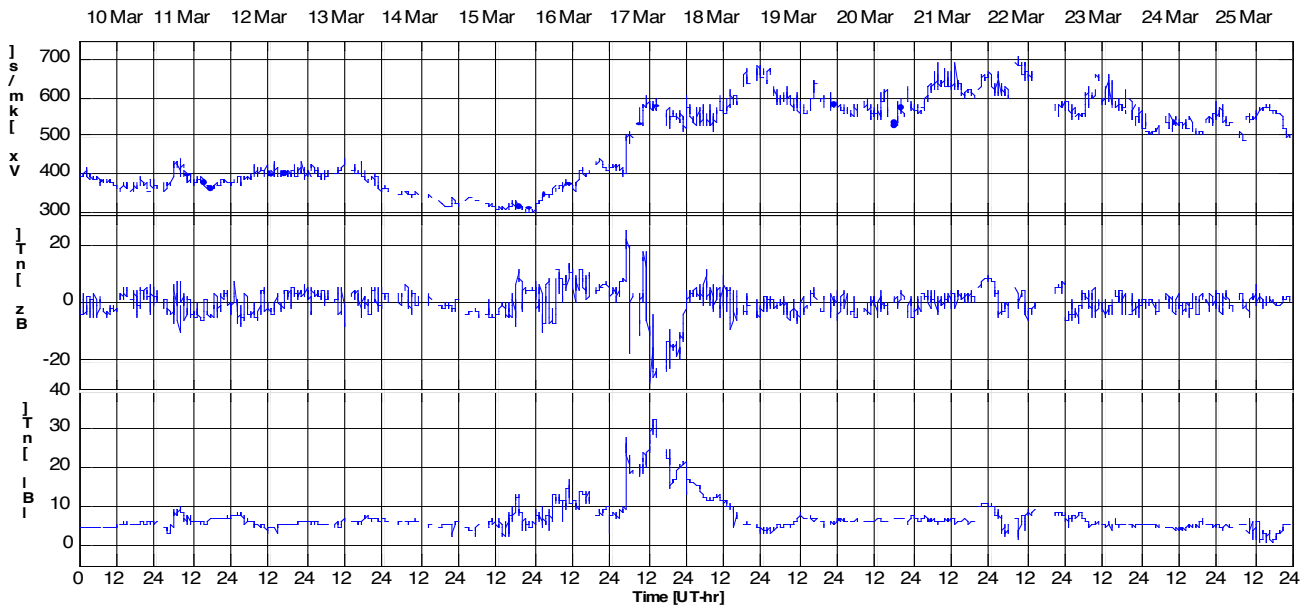

Figure 3(a): Variations of solar wind speed Vx, IMF Bz and average magnetic field |B|.

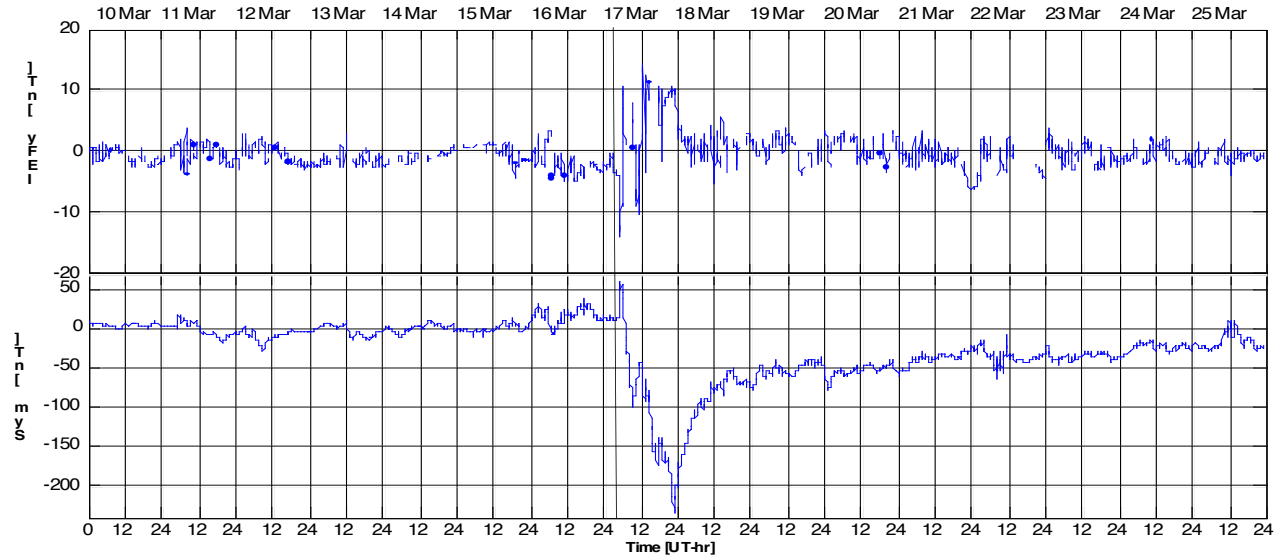

Figure 3(b): Variations of IMF B_z, Interplanetary electric field (IEF) and SYM-H for the period 10 to 25 March 2015. The black line shows the time of the sudden storm commencement.

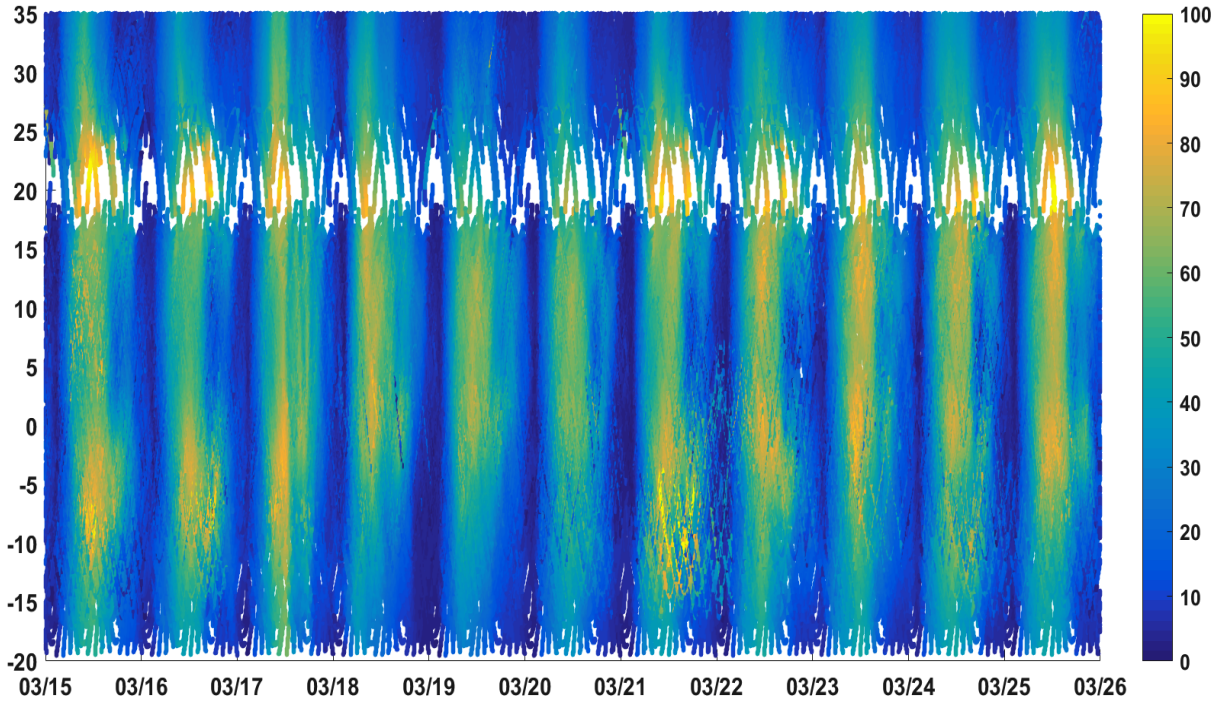

Figure 4: Total Electron Content (TEC) variations during the period 15 to 25 March 2015. The plots represents the vertical TEC at the Ionospheric Pierce Points of every satellite for every pass every day reporting on y axis the geographic latitudes and on x axis the time in UT. The white part of the graph represents a lack of data around the period and the color bar is in units of TECU.

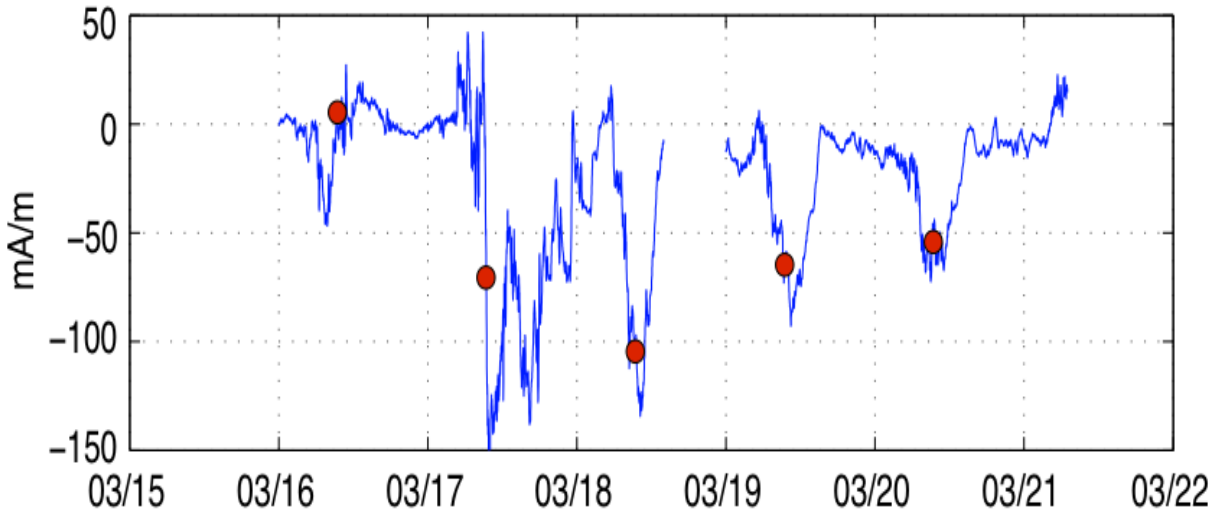

Figure 5: Eastward ionospheric disturbance currents during the period 16 to 20 March 2016. The red dots indicate midday values. The gap just before 19 March is due to an absence of data.

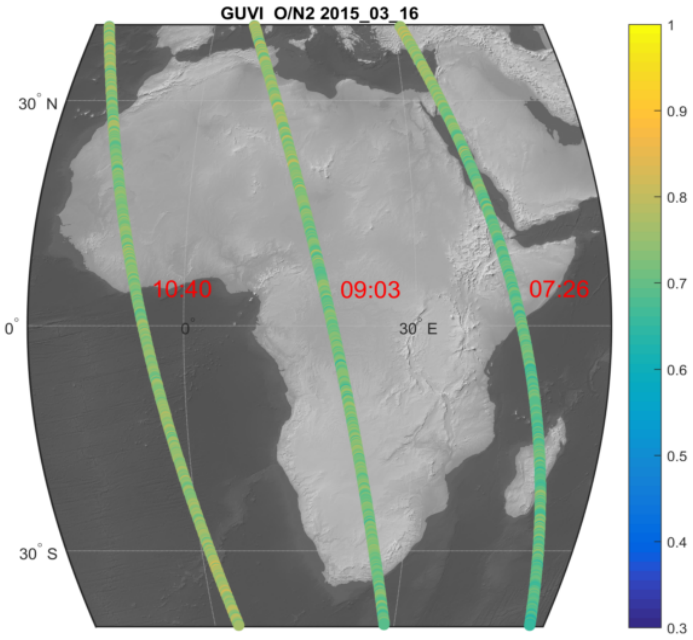

Figure 6(a):

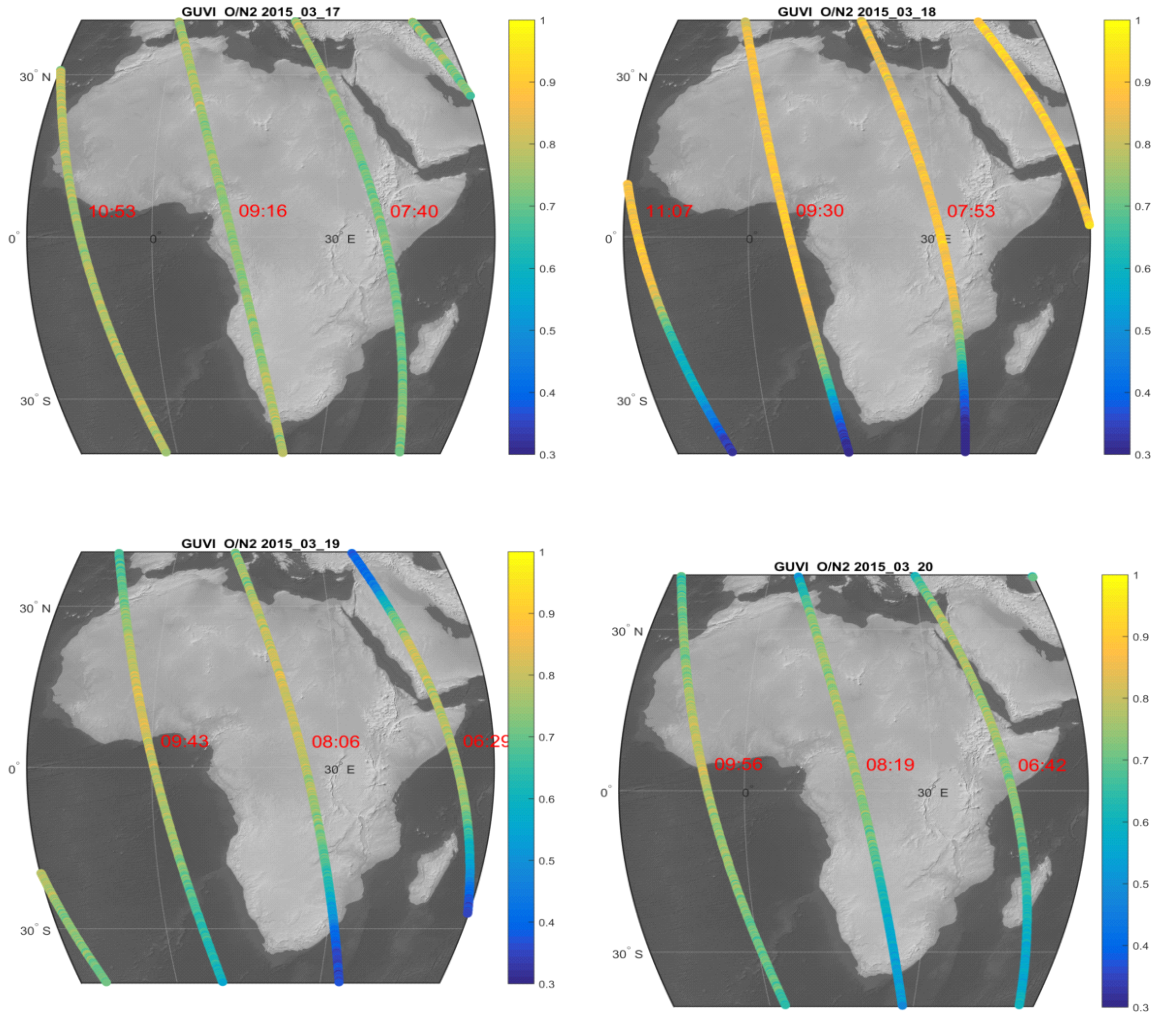

Figure 6(b):

Figure 6(a-b): Plots of the [O/N_2]-ratio during the satellite pass over the African sector for 5 days which include a day prior to the storm on the 16 March (Figure 5(a)) and 4 days during the storm of 17-20 March 2015. The color bars represent the [O/N_2]-ratio.